A COMPARISON OF DIFFERENT NUMERICAL APPROACHES FOR CALCULATING A MARTIAN ENTRY FLOW

E. Chabut, J.C. Lengrand
Laboratoire d'Aérothermique du Centre National de la Recherche Scientifique (CNRS), Orléans, France,

T.G. Elizarova
Institute for Mathematical Modeling, Russian Academy of Sciences, Moscow, Russia

M.E. Sokolova
Faculty of Physics, M.V. Lomonosov Moscow State University, Moscow, Russia

The present work is related to the aerocapture phase of the Mars Sample Return (MSR) mission, as it was planned jointly by CNES and NASA. Although the project has been cancelled, this work has an interest for any future entry problem. During the aerocapture, the MSR Orbiter (MSRO) passes through the Martian atmosphere, which decreases its velocity and allows it to orbit the planet. Its altitude first decreases, changing the flow regime from free molecular (FM) to transitional and to continuum. Then the altitude increases again, changing the regime back to transitional and FM. The purpose of the present work is to investigate the level of modeling and simplification that is acceptable in estimating the heat transfer rate received by the orbiter.

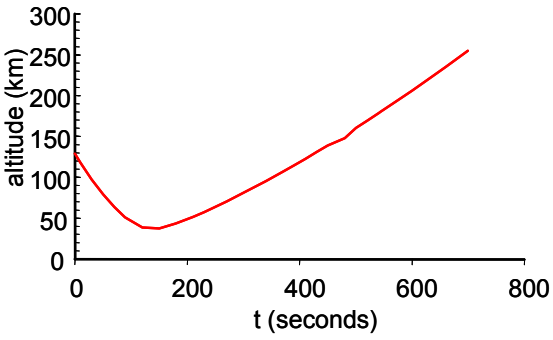

Fig.1. Typical MSRO trajectory

Flow conditions

A typical trajectory was retained (Fig.1). A simplified MSRO geometry was considered (Fig.2, left). The diameter of the orbiter and the nose radius of curvature were equal to 3.4 m and 1 m, respectively. A number of calculations were based on even simpler bodies, namely an infinitely thin disk oriented perpendicular to the freestream and a bluff-faced cylinder, whose diameters were equal to that of the orbiter. For

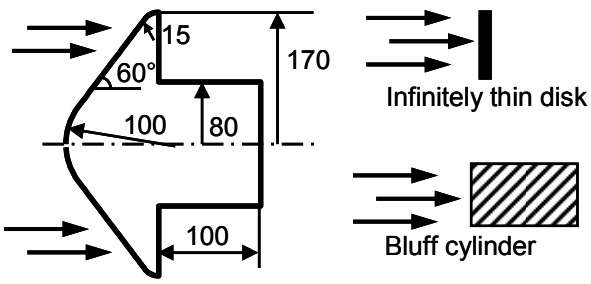

Fig. 2: Simplified geometries (dimensions in cm)

Table 1

t (s)	Z (km)	ρ (kg/m^3)	T (K)	u (m/s)	Ma	a (m/s)	μ_{VHS} (Pa.s)	Re	Kn
50	79	$1.32\ 10^{-6}$	149	5762	29.0	198	$1.22\ 10^{-5}$	1070	$3.66\ 10^{-2}$
150	38	$3.84\ 10^{-4}$	141	4285	22.2	193	$1.18\ 10^{-5}$	238000	$1.25\ 10^{-4}$
270	70	$4.26\ 10^{-6}$	154	3607	17.9	202	$1.24\ 10^{-5}$	2110	$1.14\ 10^{-2}$
300	81	$1.02\ 10^{-6}$	148	3593	18.1	198	$1.21\ 10^{-5}$	514	$4.74\ 10^{-2}$
340	95	$1.74\ 10^{-7}$	151	3578	17.9	200	$1.23\ 10^{-5}$	86.4	$2.8\ 10^{-1}$
390	114	$1.49\ 10^{-8}$	154	3559	17.6	202	$1.24\ 10^{-5}$	7.27	3.26

the purpose of the present discussion, a number of trajectory points were selected. The corresponding flow parameters are given in Table 1, where t is the physical time (from an arbitrary origin), z the altitude. The freestream is characterized by ρ (density), T (temperature), u (velocity). The other quantities in Table 1 are Ma (Mach number), a (speed of sound), μ (viscosity), Re (Reynolds number), Kn (Knudsen number). They are estimated for pure CO_2, characterized by a specific heat ration $\gamma = 1.4$ (vibrational energy not excited) and a power-law viscosity temperature relationship

$$\mu = 5.099 \times 10^{-7} T^{0.634} \qquad (1)$$

(S.I. units) fitted to the actual CO_2 viscosity at T_w = 1500 K, a temperature retained somewhat arbitrarily for the orbiter wall. The latter viscosity law is consistent with the parameters of the Variable Hard Sphere (VHS) model used to describe intermolecular interactions in the Monte Carlo (DSMC) simulations. The characteristic length retained for Re and Kn is the MSRO radius $D/2$. Kn is defined as $Kn = \lambda/(D/2)$, where the freestream mean free path λ is equal to

$$\lambda = \frac{2(7-2\omega)(5-2\omega)}{15\pi^{1/2}} \frac{\mu(T)}{\rho\left(2RT\right)^{1/2}}, \qquad (2)$$

an expression given by Bird [1] for VHS molecules. Here R denotes the perfect-gas constant per unit-mass.

Based on criteria exposed in detail in [2], the continuum flow regime is expected to hold from $t = 90$ s to $t = 210$ s and the FM regime is expected to hold for $t > 540$ s. Different methods, appropriate to the different regimes, have been used to predict the rate of heat transfer q received by the vehicle.

Numerical approaches

Unless otherwise specified, the gas is considered as pure CO_2, with no vibrational excitation and no dissociation.

Boundary Layer integral method

An integral method, based on laminar boundary layer (BL) equations has been applied along the forward-facing side of the simplified orbiter. The evolution of the thermal BL thickness Δ, is obtained by solving

$$(\Delta\rho_e u_e r)_x^2 = 2\int_0^x k \frac{T_e \mu^*}{T^* \mu_e} \left(Pr^{-\frac{2}{3}} \frac{T_w - T_e}{T_e} \right)^2 \rho_e u_e r^2 \mu_e dt, \qquad (3)$$

where r is the distance to the symmetry axis, Pr is the Prandtl number, x is the abscissa along the wall (from the stagnation point), k is a constant equal to 0.2205, $()_e$ refers to the flow properties at the BL edge. The latter are estimated from the freestream properties and the local wall pressure (modified Newtonian approximation). $()^*$ refers to Monaghan's reference quantities. Denoting the specific heat at constant pressure by c_p, the local heat transfer rate is deduced from Δ at any location x by

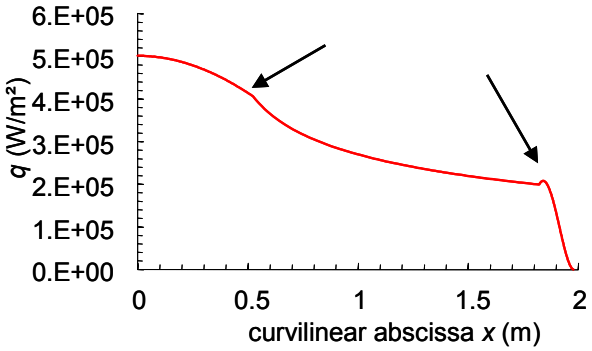

Fig.3. BL estimation of heat transfer rate at $t = 118$ s

$$q = \frac{kT_e\mu^*}{T^*\mu_e}\left(Pr^{-2/3}\frac{T_w - T_e}{T_e}\right)^2 \frac{c_p\ T_e\ \mu_e}{\Delta} \qquad (4)$$

As an example, the distribution of q is given in Fig.3 for the trajectory point where it is close to its maximal value. The slope discontinuities indicated by arrows correspond to changes in the wall radius of curvature R_n. For large abscissas, the validity of the Newtonian approximation fails because of the entropy layer. Therefore the results are questionable for abscissas larger than, say, 1 m.

The time evolution of the stagnation point heat transfer is plotted in Fig. 4. In its expected range of validity (90 s $< t <$ 210 s), it differs by less than 10% from the Sutton-Graves estimation [3], the difference being approximately 3% at the maximum.

Dieudonné [4] calculated a heat transfer rate $q = 386$ kW.m^{-2} at $t = 115$ s along a trajectory slightly different from the present one. He used a full Navier-Stokes (NS) simulation,

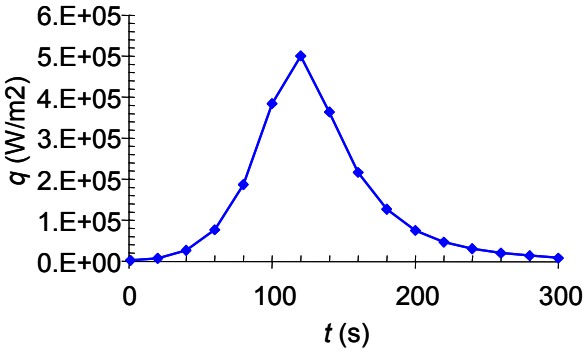

Fig.4. Time evolution of stagnation point heat transfer (BL estimation)

taking into account "hot gas" effects and assuming full recombination of CO_2 at the wall. Assuming a non-catalytic wall, he found q =121 kW.m^{-2} at the same point.

Applying the present BL integral method to Dieudonné's flow parameters results in $q = 485$ kW.m^{-2}. The difference with the NS-catalytic result is rather small, when considering the uncertainty on wall catalycity.

Quasigasdynamic (QGD) equations

The problem was also investigated using a continuum approach – quasigasdynamic (QGD) equations, developed by one of the authors (TGE) and her co-workers. They are presented, e.g., in [5] [6]. They differ from Navier-Stokes (NS) equations by additional terms in the conservation equations. Those terms are proportional to $\tau = \mu / p \approx \tau_c$, where p is the pressure and τ_c the local mean time between molecular collisions. Their origin is connected to the non-Maxwellian character of the velocity distribution function. QGD equations reduce to NS ones for vanishing local Knudsen numbers, the difference being O(Kn) (or O(Kn^2) for stationary flows). Thus they can be regarded as an approximation of NS ones. q is obtained by the same expressions in NS and QGD models. QGD equations were applied to the bluff-cylinder geometry. τ was taken as

$$\tau = \frac{A\ T^{\omega}}{p\ Sc} + \left(\frac{\alpha\ h}{a}\right), \text{ where } h = \sqrt{h_r^2 + h_z^2} \qquad (5)$$

A and ω are the coefficients of the viscosity law in Eq.(1). Sc is the Schmidt number. h refers to space discretization and α is a coefficient that ensures the stability of the calculation. In the present context, the QGD formalism is essentially used to introduce an artificial viscosity.

A number of trajectory points were considered. The corresponding grids and artificial viscosity coefficients are given in Table 2.

Velocity slip and temperature jump were introduced in the boundary conditions, assuming full accommodation at wall temperature :

Table 2

t(s)	Grid	$h/(D/2)$	α
50	80x60	0.05	0.1
150	240x240	0.0125	0.5
270	160x120	0.025	0.2
300	160x120	0.025	0
340	40x30	0.1	0

$$u_s = \frac{\sqrt{\pi}\cdot\mu}{\rho\cdot\sqrt{2RT}}\cdot\frac{\partial u_\tau}{\partial n} \qquad (6)$$

$$T_s - T_w = \frac{\sqrt{\pi}}{2\cdot R}\cdot\frac{1}{\sqrt{2RT}}\cdot\frac{\kappa}{\rho}\cdot\frac{\partial T}{\partial n} \qquad (7)$$

where n refers to the normal to the wall, κ is the thermal conductivity and u_τ the tangential velocity. The flow properties as well as wall quantities (including the heat transfer rate) have been obtained for different test-cases.

QGD results are sensitive to grid refinement and to artificial viscosity, as seen in Fig.5. QGD curves are labeled by values of $h/(D/2)$ and α. As these parameters tend to zero, QGD results become consistent with those labeled as DISIRAF, a DSMC calculation that can be considered as a reference and will be presented later. Examples of flowfields obtained by the QGD equations are presented in Fig.6.

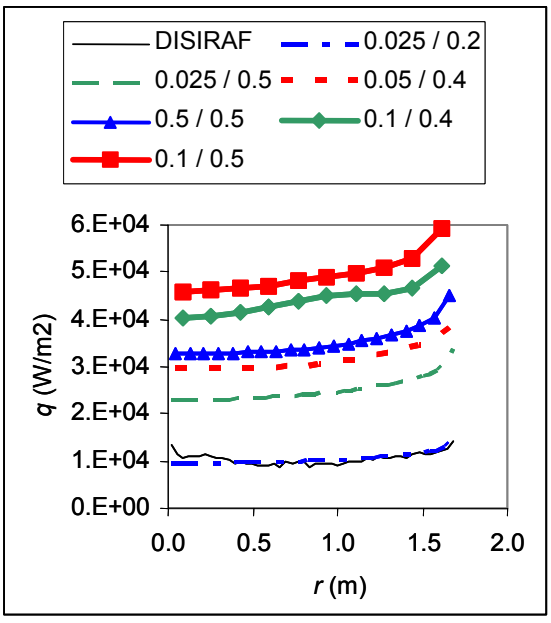

Fig. 5. Grid convergence (QGD, t = 270 s)

Direct Simulation Monte Carlo method

DSMC is a simulation at a molecular level that is free from the hypothesis of near-equilibrium. It is widely used as a tool for treating flows in the transitional regime. The basis of the method is described in [1]. How it has been applied to the present problem is described in [2]. Here we just recall the results for the purpose of comparison with other methods. Three DSMC codes have been used.

DISIRAF (DIrect SImulation of RArefied Flows) has been developed by one of the authors (JCL). It treats non-reactive mixtures of VHS molecules. Rotational energy is allowed, vibrational energy is not.

DS2G has been developed by G.A. Bird. It is available free of charge on the internet. It al-

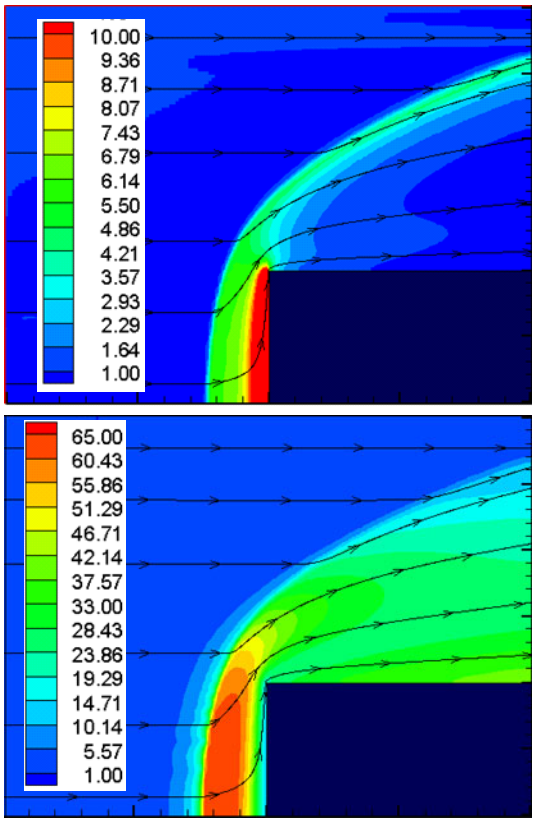

Fig.6. QGD flowfield at t = 270 s - non-dimensional density (upper) and temperature (lower)

lows for reactive gas mixtures and vibrational excitation. It computes 2D and axisymmetric flows. It is associated with a library of gas properties that includes "cold" CO_2 and reactive air, but not reactive CO_2.

DS2V is a commercial DSMC code developed by G.A. Bird. At the time when this work was carried out, it allowed for reactive gas mixtures and vibrational excitation. It allowed for 2D and axisymmetric "wind-tunnel like" flows. It was associated with a library of gas properties that included "cold" CO_2 and a reactive Martian atmosphere.

Flow properties as well as wall quantities (including the heat transfer rate) have been obtained for different test-cases. DS2G and DS2V have been applied to the simplified orbiter geometry and to the perpendicular disk geometry, whereas DISIRAF has been applied only to the disk. Because the underlying modeling is less restrictive than that of continuum methods, DSMC results can be considered as references, provided the validity conditions (in terms of space and time discretization) be fulfilled.

Free-molecular flow calculation

Under the FM regime assumption, the front face of the vehicle receives molecules directly from the freestream. If they were re-emitted diffusely with full accommodation, they would seem to emanate from a gas at rest, whose temperature is T_w and whose density is adjusted to ensure equal numbers of incident and re-emitted molecules. Let s denote the molecular speed ratio ($s = u/(2RT)^{1/2}$). If the incoming flow is hypersonic ($s >> 1$), the resulting energy transfer q is equal to

$$\frac{a\rho u^3}{2s^2}\left(s^2+\frac{\gamma}{(\gamma-1)}-\frac{(\gamma+1)T_w}{2(\gamma-1)T}\right)\cos\theta, \quad (8)$$

where θ is the angle between the direction of the freestream velocity and the normal to the wall ($\cos\theta = 1$ at the stagnation point). a is the accommodation coefficient for energy ($a = 1$ for full accommodation). Heat transfer is proportional to a and does not depend on the radius of curvature. It does not depend on any transport property (e.g., viscosity law).

Discussion of "cold gas" results

The discussion is based on the values of the stagnation point heat transfer rate, obtained under the cold gas hypothesis by the above-described methods and plotted in Fig. 7. The QGD results agree well with the DISIRAF ones at $t = 50$ and 270 s. They lie above the BL ones at $t = 150$ s, probably due to insufficient grid convergence.

The influence of a number of physical parameters has been studied.

Viscosity. Comparisons between methods make sense only if consistent models of viscosity (or molecular interaction) are used. BL computations have been carried out with a Sutherland-like viscosity law fitted to tabulated data (handbook). They have been repeated with a power-law ($\mu \sim T^{\omega}$) fitted to the previous one at $T_w = 1500$K. The results can hardly be distinguished in Fig.7 (this is not true when the power-law is fitted at a different temperature, e.g. the free-stream temperature). All DSMC calculations were based on a VHS model, consistent with a power-law viscosity. The parameters chosen for the VHS model were consistent with the fit at 1500 K. However the DS2V calculation at $t = 340$ s was repeated with the parameters taken from the library of the code. No difference is observed in the results. This confirms the consistency of models for viscosity and molecular interaction used in this work.

Accommodation. In the FM regime, the heat transfer rate is simply proportional to the accommodation coefficient (Eq. (8), free-molec. in Fig.7). The influence of accommodation should decrease when the continuum regime is approached, as it is not part of the classical NS equations. This is confirmed by DSMC calculations (see DISIRAF results for $a = 1$ and 0.5 in Fig.7).

Geometry. In the FM regime, the heat transfer rate does not depend on the vehicle ge-

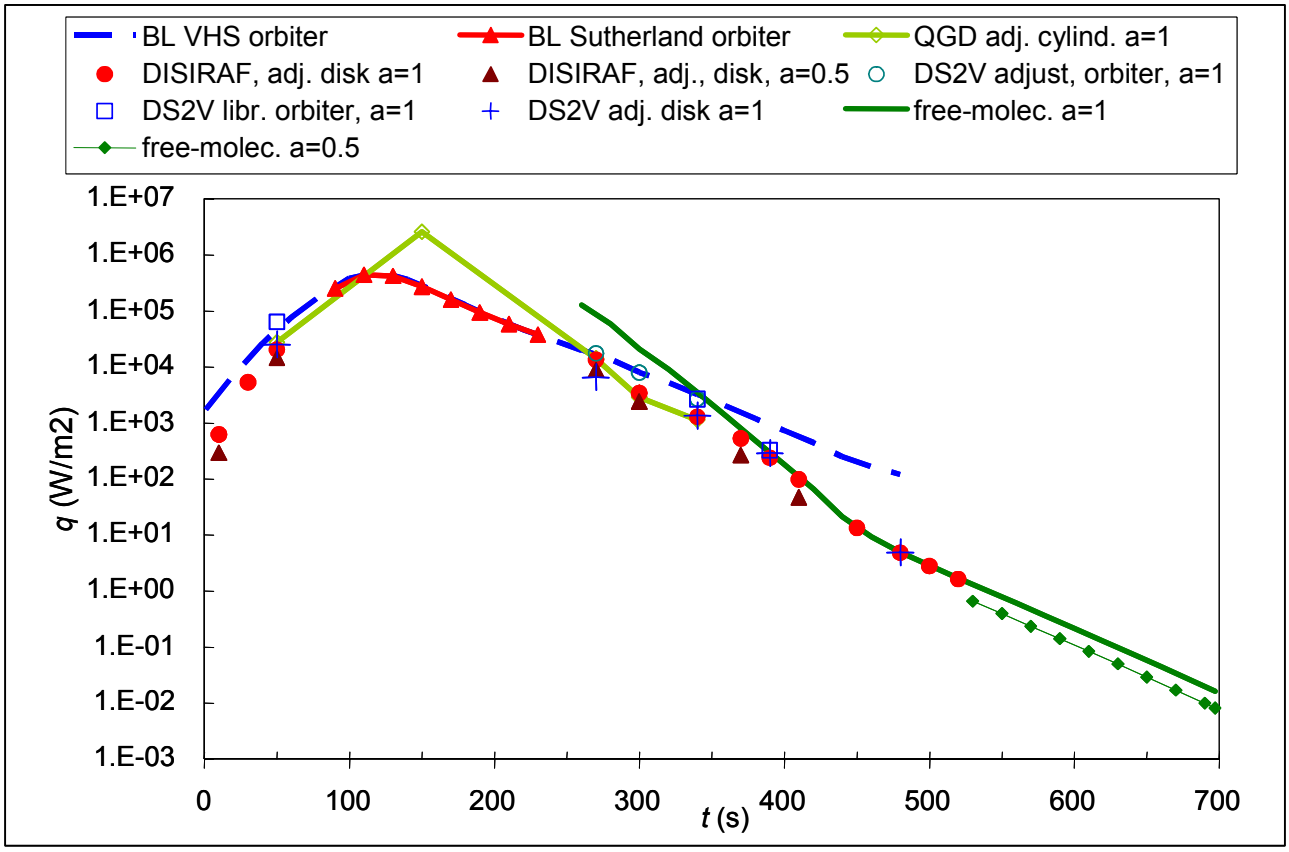

Fig. 7. Heat transfer rate at stagnation point

ometry. The influence of geometry should increase as the continuum regime is approached (q becomes proportional to $R_n^{-1/2}$). This is confirmed by DSMC calculations (DS2V results in Fig.7).

The BL and FM approaches have been applied far beyond their expected ranges of validity and their results are plotted in Fig. 7. An interesting result of the present work is that the heat transfer rate in the transitional regime does not lie between the extrapolated continuum and FM limits, which is in contradiction with the widely-used interpolation methods, known as "bridging methods". If we consider the heat transfer rate only for the orbiter geometry we note that it is nearly equal to the BL or FM values, whichever is smaller.

"Hot gas"

The DS2V code has been applied to the orbiter geometry. Vibrational excitation, dissociation, recombination and wall catalycity were taken into account by using the "Martian atmosphere" library models. A parametric study has been conducted, by varying wall catalycity, accommodation of vibrational energy, vibrational relaxation parameter Z_v and the point along the trajectory.

As examples, distributions of translational temperature, vibrational temperature and CO_2 mole fraction at t = 50s are shown in Fig. 8.

All heat transfer results remain close to their cold gas values. However, in the descent phase, chemistry tends to decrease q and wall catalycity tends to increase it. In the ascent phase the role of chemistry is negligible because the flow energy is too low to induce dissociation.

Compared with a cold gas simulation, taking into account vibration (with partial or full accommodation) increases the energy of re-emitted molecules, which decreases q.

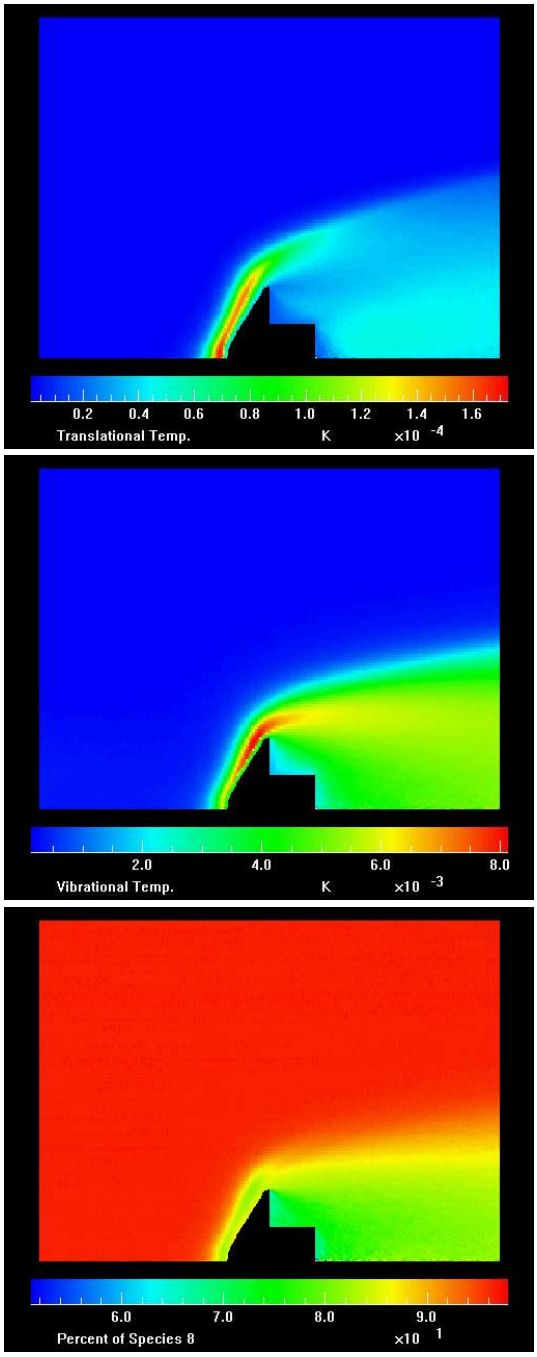

Fig.8. Flowfield at t = 50 s: From top to bottom: translational temp., vibrational temp., CO_2 mole fraction

Small values of Z_v are favorable to vibrational excitation in the flow. This reduces the energy exchange with the wall in the case of partial or zero vibrational accommodation.

Conclusion

A detailed parametric study of heat transfer to the MSRO entering a Martian atmosphere has been carried out, with main emphasis put on the transitional regime.

The cold gas approximation appears to be an acceptable one. The boundary layer, QGD and free-molecular approaches are valid in a rarefaction range much larger than expected. The well-known "bridging methods" seem to be inadequate in the present case.

In addition, the influence of parameters that describe the "hot gas" behavior has been investigated and reported in the paper.

Acknowledgment

CNES and CNRS supported jointly the Ph. D. grant of one of the authors (EC).

References

[1] Bird G.A. *Molecular gas dynamics and the simulation of gas flows*. Clarendon Press, Oxford, 1994

[2] Chabut E., Lengrand J.C. Simulation of a hypersonic flow during a Mars entry. *Proc. 3rd Intern. Symposium on Atmospheric Reentry Vehicles and Systems*, Arcachon (Fr), 24-27 March 2003, pp.526-534, 2004.

[3] Couzi J. et al. Netlander aerothermal data dase derivation, *Proc. 3rd Intern. Symposium on Atmospheric Reentry Vehicles and Systems*, Arcachon (Fr), 24-27 March 2003, pp.37-45, 2004.

[4] Dieudonné W. Numerical MSRO rebuilding of ground facilities campaigns and flight aerocapture predictions, *Proc. 3rd Intern. Symposium on Atmospheric Reentry Vehicles and Systems*, Arcachon (Fr), 24-27 March 2003, pp.545-553, 2004.

[5] Elizarova T.G. et al. Rarefied gas flow simulation based on quasigasdynamic equations. *AIAA J.*, Vol.33, pp. 2316-2324, 1995

[6] Elizarova T.G., Sheretov Yu.V. Theoretical and numerical analysis of Quasi-Gasdynamic and Quasi-Fluid-Dynamic Equations. *Comp. Math. and Math. Phys*, Vol. 41, No 2, pp.219-234, 2001.